Robust direct differentiation and maturation of human pluripotent stem cells to hepatocyte-like cells

Ken-ichiro Kamei,[1,*] Momoko Yoshioka,[1] Shiho Terada,[1] Yumie Tokunaga[1] and Yong Chen[1,2]

[1] *Institute for Integrated Cell-Material Sciences (WPI-iCeMS), Kyoto University, Yoshida-Ushinomiya-cho, Sakyo-ku, Kyoto 606-8501, Japan*

[2] *Ecole Normale Supérieure, CNRS-ENS-UPMC UMR 8640, 24 Rue Lhomond, Paris 75005, France*

*Corresponding author.

E-mail address: kkamei@icems.kyoto-u.ac.jp (K. Kamei)

Abstract

Functional hepatocytes are needed for drug screening and chemical-safety testing, and primary hepatocytes are commonly used, despite problems involving donor limitations, lot-to-lot variation, and unsatisfactory two-dimensional culture methods. Human pluripotent stem cells (hPSCs) might be a strong contender to address the aforementioned issues; however, there remain technological challenges involving the robust, highly efficient production of high-purity hepatic clusters. Here, we developed a method to accurately control hepatic differentiation by first inhibiting the phosphoinositide 3-kinase- and Rho-associated protein kinase-signaling pathways to stop self-renewal and improve survival, respectively, which enabled formation of a well-defined endoderm and facilitated hepatocyte commitments. Additionally, we optimized hepatic induction and differentiation of hPSCs by adjusting step-by-step timing and used a microfluidic device to create a three-dimensional (3D) culture environment that enhanced the maturation and function of hepatocyte-like cells by increasing the expression of both hepatic maturation markers and cytochrome P450. Furthermore, we confirmed improvements in drug uptake/excretion capabilities in >90% of 3D-maturated hepatocyte-like cells by indocyanin green assay. Our results indicated that this approach for generating 3D microscale hepatocytes could enhance the processes involved in drug screening and chemical-safety testing.

Introduction

Hepatocytes constitute the majority of cells in the liver and have recently received attention for their use in drug screening and toxicological testing. Although the importance of hepatocytes is increasing, issues remain concerning their application. Primary hepatocytes can be obtained from healthy donors; however, these cells cannot proliferate under standard cell-culture conditions and often experience loss of function. To overcome this, established cell lines are used for cell culture and *in vitro* drug testing, although these cells are often originally harvested from tumors and do not represent healthy liver functions. Therefore, the necessity to establish an *in vitro* drug test using liver cells requires functional variants.

To meet this requirement, human pluripotent stem cells (hPSCs), such as embryonic and induced pluripotent stem cells [hESCs (1) and hiPSCs (2), respectively] hold great potential as sources to generate hepatocytes. hPSCs exhibit two distinctive functions: unlimited self-renewal without karyotypical abnormality and the ability to differentiate into almost any cell type. Therefore, hPSCs allow for the generation of sufficient amounts of target cells for cell transplantation and drug screening.

However, there remain issues with current methods related to the induction of hepatic differentiation from hPSCs resulting in functional and mature hepatocytes. These methods involve 1) formation of embryoid bodies or cell aggregates (3), or 2) introduction of exogenous genes [e.g., *HHEX* (4) and *SOX17* (5)]. Unfortunately, these methods might often cause quality control difficulty involving differentiated cells, and safety concerns, such as tumorigenesis induced by transplanted cells in a patient. Moreover, conventional differentiation processes do not allow for the use of dissociated cells. Therefore, it is necessary to establish a novel method enabling the efficient and robust differentiation of hPSCs into functional hepatocytes.

The timing of hepatic differentiation from hPSCs also requires consideration due to the time required for hepatocyte-like cell maturation. Because embryonic hepatic development is a precisely regulated, time-sensitive process, movement to subsequent steps of differentiation needs to be

carefully regulated in order to ensure that differentiating hPSCs are able to continue further differentiation.

Cell culture method also requires new innovation. For long time, 2D culture of hepatocytes has been carried out, but also problematic. In the case of primary hepatocytes, they often lost their function under 2D culture (6). Therefore, a number of reported suggested to use 3D culture methods to make hepatocyte more functional. Moreover, recent studies showed that organoids (7, 8) hold a promise to obtain more functional micro live tissues that that of 2D culture. However, in the aforementioned methods, each cell aggregates and organoids showed the different size and structure resulting low reproducibility, since they are relied on only the stem cells capability for tissue formation. Therefore, these methods have still not reach to the stage for drug screening.

Here, we developed a protocol enabling the efficient differentiation of hepatocyte-like cells from hPSCs resulting in high degrees of purity and reproducibility (**Fig. 1**). To facilitate efficient hepatic differentiation and cell survival, our method utilizes a cocktail of chemicals and growth factors. Additionally, we were able to derive robust hepatic differentiation by using dissociated hPSCs rather than hPSC aggregates or clumps, while still maintaining a high cell-survival rate. Moreover, our method does not require the use of exogenous genes, thereby eliminating concerns of genetic integration into host cells and variations in gene-delivery efficiency. Furthermore, to accomplish hepatocyte maturation, we applied a microfluidic three-dimensional (3D) cell-culture platform (9, 10). Our results indicated that this method allowed for the acquisition of large amounts of functional hPSC-derived hepatocytes.

Materials and Methods

hPSC culture

Human ESCs (hESCs) were used according to the guidelines of the ethnical committee of Kyoto University. Prior to culturing, hESC-certified Matrigel (Corning, Corning, NY, USA) was diluted with Dulbecco’s modified Eagle medium (DMEM)/F12 medium (Sigma-Aldrich, St. Louis, MO,

USA) at a 1:75 (v/v) ratio and coated onto a culture dish. Matrigel was incubated in a dish for 24 h at 4°C. Excess Matrigel was removed, and the coated dish was washed with fresh DMEM/F12 medium.

We used mTeSR-1-defined medium (Stem Cell Technologies, Vancouver, Canada) for daily culturing of H9 hESCs and 253G1 hiPSCs, and for passaging, cells were dissociated with TrypLE Express (Life Technologies, Carlsbad, CA, USA) for 3 min at 37°C and harvested. A cell strainer was used to remove undesired cell aggregates from the cell suspension, and cells were centrifuged at 200 × *g* for 3 min and resuspended in mTeSR-1 medium. Cells were counted using a NucleoCounter NC-200 (Chemetec, Baton Rouge, LA, USA). mTeSR-1 medium containing 10 μM of the Rho-associated protein kinase (ROCK) inhibitor Y-27632 (Wako, Osaka, Japan) was used to prevent apoptosis of dissociated hPSCs on day 1. mTeSR-1 medium lacking the ROCK inhibitor was used on subsequent days, with daily medium changes.

Hepatic differentiation from hESCs

Prior to inducing differentiation, a cell-culture dish was coated with 0.1% gelatin in phosphate-buffered saline (PBS) at 25°C room temperature for 30 min. The gelatin solution was then aspirated, and DMEM/F12 medium (Sigma-Aldrich) supplemented with 10% (v/v) fetal bovine serum (FBS), penicillin/streptomycin, and 100 μM β-mercaptoethanol (Sigma-Aldrich) was introduced onto the culture dish for serum coating at 37°C for 24 h. The coated dish was then rinsed with fresh medium.

To induce endoderm differentiation, cultured hESCs were washed with PBS and treated with TryPLE Express at 37°C for 5 min, followed by the addition of basal medium and transfer of the cell suspension into a 15-mL tube. Cells were centrifuged at 200 × *g* for 3 min, and the supernatant was removed. Cells were resuspended in mTeSR-1 or TeSR-E8 medium supplemented with 10 μM Y27632 and 100 ng mL^{-1} activin A, plated on a serum-coated culture dish, and cultured in a humidified incubator at 37°C with 5% CO_2 for 24 h. At the end of day 1, the medium was replaced

with fresh mTeSR-1 medium supplemented with 10 μM Y27632 and 100 ng mL^{-1} activin A and cultured for another 24 h. On day 2, the medium was replaced with mTeSR-1 medium supplemented with 10 μM Y27632, 100 ng mL^{-1} activin A, 10 ng mL^{-1} bone morphogenetic protein (BMP)-4, 10 μM LY294002, and 3 μM CHIR99021, and cells were incubated for 24 h. On day 3, medium was replaced with mTeSR-1 medium supplemented with 10 μM Y27632, 100 ng mL^{-1} activin A, 10 ng mL^{-1} BMP-4, and 10 μM LY294002, and cells were incubated for 24 h. On day 4, medium was replaced Roswell Park Memorial Institute (RPMI) medium supplemented with B-27 (Life Technologies), 100 ng mL^{-1} activin A, and 100 ng mL^{-1} basic fibroblast growth factor (bFGF), and cells were incubated for 24 h.

To induce anterior definitive-endoderm (DE) specification, cells were treated with RPMI medium supplemented with 50 ng mL^{-1} activin A, with daily medium changes for 3 days. Cells were then treated with RPMI medium supplemented with 20 ng mL^{-1} BMP-4 and 10 ng mL^{-1} fibroblast growth factor-10, with daily medium changes for 4 days.

On day 12, the medium was replaced with hepatocyte basal medium (Lonza, Basel, Switzerland) supplemented with 30 ng mL^{-1} oncostatin M and 50 ng mL^{-1} hepatocyte growth factor to induce maturation of the differentiated hepatocytes. Cells were incubated at 37°C, and medium was changed every 2 days.

HepG2 cell culture

HepG2 cells were cultured with DMEM supplemented with 10% (v/v) FBS, 1% P/S, and 1 mM nonessential amino acids, and the medium was changed every 2 to 3 days. The cells were passaged with trypsin-EDTA solutions at a 1:~10 to 1:~20 subculture ratio.

Flow cytometry

Cells were harvested with TrypLE Express and rinsed with PBS twice prior to cell counting. For staining with antibodies, cells were diluted to a final concentration of 1×10^7 cells mL^{-1} in PBS

supplemented with 2% fetal calf serum (FCS). Fluorescence-labeled antibodies were added and incubated at room temperature for 30 min. As a negative control, specific isotype controls were used. After removing excess antibodies by centrifugation at 300 × *g* for 5 min, cells were washed with PBS containing 2% FCS, and cell suspensions were applied to a FACS Canto II (BD Biosciences, Franklin Lakes, NJ, USA) for flow cytometric analysis. Data analysis was performed using FlowJo software (v9; FlowJo, LLC, Ashland, OR, USA).

Reverse transcription-polymerase chain reaction (RT-PCR)

Total RNA was purified using an RNeasy Mini Kit (Qiagen, Hilden, Germany), and 1 µg of total RNA was reverse transcribed to generate cDNA using PrimeScript RT master mix (Perfect Real Time; Takara Bio, Shiga, Japan). A reaction mixture (25 µL) containing 1 µL cDNA, 0.2 µM PCR primers (**Supplementary Table S1**), and 5 U of Taq DNA polymerase (Takara Bio) was applied to a thermal cycler (Applied Biosystems 7300 real-time PCR system; Applied Biosystems, Foster City, CA, USA). PCR was performed with 30 to 35 cycles (94°C for 30 s, 58°C for 30 s, and 72°C for 60 s). Ten microliters of PCR product was electrophoresed on 1.2% agarose gels and visualized by GelRed nucleic acid staining (Biotium, Fremont, CA, USA).

Quantitative RT-PCR array

The cDNA obtained in solution was mixed with SYBR Premix Ex Taq II (Tli RNaseH Plus; Takara Bio) and introduced into the hepatocyte-specific genes in a 96-well plate according to manufacturer instructions (PrimerArray hepatic differentiation (human); Takara Bio) (**Supplementary Table S2**). PCR conditions included an initial incubation at 95°C for 30 s, followed by 40 cycles of 95°C for 5 s and then 60°C for 31 s on a 7300 real-time PCR system (Applied Biosystems).

Immunocytochemistry

Cells were fixed with 4% paraformaldehyde in PBS for 20 min at 25°C and then permeabilized with 0.5% Triton X-100 in PBS for 16 h at 25°C. Subsequently, cells were blocked in PBS (5% normal goat serum, 5% normal donkey serum, 3% bovine serum albumin, 0.1% Tween-20) at 4°C for 16 h and then incubated at 4°C for 16 h with the primary antibody [anti-human α1 anti-trypsin (A1AT) rabbit IgG, 1:800; Dako, Glostrup, Denmark] in PBS with 0.5% Triton X-100. Cells were then incubated at 37°C for 60 min with a secondary antibody (AlexaFluor 488 Donkey anti-rabbit IgG, 1:1000; Jackson ImmunoResearch, West Grove, PA, USA) in blocking buffer prior to a final incubation with 4′,6-diamidino-2-phenylindole (DAPI) at 25°C for 30 min.

Image acquisition

The sample containing cells was placed on the stage of a Nikon ECLIPSE Ti inverted fluorescence microscope equipped with a CFI plan fluor 10×/0.30 N.A. objective lens (Nikon, Tokyo, Japan), CCD camera (ORCA-R2; Hamamatsu Photonics, Hamamatsu City, Japan), mercury lamp (Intensilight; Nikon), XYZ automated stage (Ti-S-ER motorized stage with encoders; Nikon), and filter cubes for fluorescence channels (DAPI and GFP HYQ; Nikon). For image acquisition, the exposure times were set at 500 ms for DAPI and 500 ms for GFP HYQ (for A1AT).

Indocyanine green (ICG) uptake/excretion assay

Briefly, 1 mg mL^{-1} of ICG was dissolved in hepatocyte-maturation medium, and cells were treated with ICG solution for 1 h, rinsed with hepatocyte-maturation medium, and then observed using a bright-field microscope (Olympus, Tokyo, Japan). After 24 h, cells were observed again to visualize excretion capability.

Microfluidic device fabrication

A microfluidic device was fabricated using stereolithographic 3D-printing techniques and solution cast-molding processes (10). The mold for the microfluidic channels was produced using a 3D

printer (Keyence Corporation, Osaka, Japan). Sylgard 184 polydimethylsiloxane (PDMS) two-part elastomer (10:1 ratio of pre-polymer to curing agent; Dow Corning Corporation, Midland, MI, USA) was mixed and poured into a 3D-printed mold to produce a 5-mm-thick PDMS layer. The PDMS material was then cured in an oven at 65°C for 48 h. After curing, the PDMS form was removed from the mold, trimmed, and cleaned. The PDMS form and a glass dish or plastic plate were corona-plasma-treated (Kasuga Denki, Inc., Kawasaki, Japan) and bonded together by baking in an oven at 80°C.

3D cell culture in a microfluidic device

Prior to use, a microfluidic 3D cell-culture device was sterilized in 70% ethanol and placed under ultraviolet light in a biosafety cabinet for 30 min. A microfluidic cell-culture chamber was then coated with Corning Matrigel hESC-qualified matrix (Corning) diluted to 1:75 (v/v) with DMEM/F12 (Sigma-Aldrich). After a 1-day incubation at 4°C, excess Matrigel was removed, and the coated dish was washed with fresh DMEM/F12. Cells were harvested using trypsin and collected in a 15-mL tube. Following centrifugation, cells were suspended in hepatocyte-maturation medium and introduced into a microfluidic device via a cell inlet. The microfluidic device was placed in a humidified incubator at 37°C with 5% CO_2 atmosphere, and the medium was changed daily.

Statistical gene-expression analysis

Using normalized gene-expression values for the quantitative RT-PCR array, gene clusters were generated by the Consensus Cluster algorithm in the *R* package “ConsensusClusterPlus” (11). Mean values were calculated in each cluster and for each day, and fold changes were calculated using liver values as a standard.

Results and Discussion

Cell survival and robustness of (DE) differentiation is enhanced by phosphoinositide 3-kinase (PI3K) and ROCK inhibition

Induction of DE differentiation is the most critical step required to promote further differentiation (**Figure 2**). In this process, transforming growth factor-β (12, 13), BMP-4 (14), β-catenin (15, 16), and basic fibroblast growth factor (16, 17) -signaling pathways play critical roles. Moreover, the PI3K-signaling pathway is critical for the maintenance of hPSC self-renewal (18, 19), with inhibition of this pathway resulting in hPSC differentiation. Previously, Hannan et al. (2013) established a method to effectively achieve hPSC differentiation to DE differentiation using a cocktail of activin A, BMP-4, bFGF, LY294002, and CHIR99021, but without the use of exogenous genes. However, this method results in massive cell death and inefficient and irreproducible outcomes. Furthermore, to improve robustness, the use of hPSC aggregates is unrealistic due to the challenge associated with size control, which is a critical factor for lineage determination during hPSC differentiation. Therefore, the use of dissociated hPSCs is required to improve robustness, but the related processes continue to result in large amounts of cell death.

Therefore, we used a ROCK inhibitor (Y27632), which has been used to facilitate the survival of dissociated, self-renewing hPSCs (20). We hypothesized that administration of a ROCK inhibitor would also facilitate cell survival for an early stage of DE differentiation.

For the medium, we modified mTeSR-1-defined medium (21) containing BMP-4, and bFGF (**Fig. 1** and **Supplementary Table S3**), which are also commonly used as key factors to introduce DE differentiation as aforementioned. We observed that hPSCs showed unstable behavior following introduction of the new culture conditions; therefore, it was beneficial for establishing robust differentiation protocols with the use of self-renewing culture medium at the beginning, followed by gradually changing to the differentiation medium. Therefore, activin A, BMP-4, LY294002, and CHIR99021 were added into the mTeSR-1 medium for DE differentiation.

To confirm increases in cell survival during DE differentiation, H9 hESCs (1) following 1 day of treatment were counted (**Fig. 2A**). Cells treated with both 10 μM Y27632 and 10 μM

LY294002 showed significant increases in cell number, as compared with levels observed in cells treated with only LY294002. This result indicated that inhibition of the ROCK-signaling pathway improved cell survival to a degree greater than that observed following inhibition of the PI3K-signaling pathway.

We then investigated differences in outcomes based on initiating differentiation from either dissociated or clumped hPSCs according to cell number and doubling time (**Fig. 2B and C**). We observed that following a 5-day incubation with 10 μM Y27632 and 10 μM LY294002 and DE differentiation, both dissociated and clumped hESCs increased cell numbers with similar doubling times. These results suggested that Y27632 improves the cell survival even during DE differentiation, but not proliferation.

To confirm cell status following DE differentiation, the expression of C-X-C-motif chemokine receptor-4 (CXCR4), a DE-differentiation marker, was quantitatively analyzed by flow cytometry (**Fig. 2D**) and compared with levels measured in chemically defined medium (CDM-PVA) (22) (Supplementary Table S4). Both H9 and 253G1 cells treated with mTeSR-based medium showed higher degrees of purity and enhanced CXCR4 expression (99.6%) compared to that of cells cultured in CDM-PVA medium (81.5%). We also investigated the effects of initial cell-seeding density on the induction of DE differentiation (**Fig. 2E**). During the 5-day DE differentiation, cell number in all cell densities increased ~10 fold (**Fig. 2B**); however, in terms of CXCR4 expression, the increase in initial cell number revealed bimodal cell populations (**Fig. 2F**). These results indicated that use of smaller initial cell-seeding density resulted in a more homogeneous cell population with higher CXCR4 expression. In addition to the CXCR4 cell-surface marker, we also measured expression of the sex-determining region Y box-17 (SOX17) transcription factor and endoderm-lineage marker by quantitative PCR (**Fig. 2E**). The use of cell clumps resulted in higher *SOX17* expression as compared with using dissociated cells, with *SOX17* expression subsequently decreasing along with increasing cell numbers. Although lower initial cell-seeding density (2.5×10^4 cells cm^{-2}) resulted in large variations in *SOX17* expression. We also

confirmed hepatocyte differentiation by monitoring mRNA expression of α-fetoprotein (*AFP*) and hepatocyte nuclear factor 4α (*HNF4α*) differentiation markers on day 12 (**Fig. 2F**). The use of cell aggregates with lower initial cell-seeding density (2.5×10^4 cells cm^{-2}) did not result in *AFP* and *HNF4α* expression. Based on these results, we used 5×10^4 cells cm^{-2} for further differentiation protocols due to our observation of higher purity and improved robustness at higher initial cell densities. Under the optimized conditions, we tested DE differentiation from 253G1 hiPSCs (23) and differentiation to highly pure CXCR4-positive DE cells (**Supplementary Fig. S1**).

Efficient induction of anterior DE (ADE) specification and hepatocyte commitment (HC)

We established a robust and efficient procedure for ADE specification from DE cells, as well as HCs, to generate hepatic progenitor cells (**Fig. 3 and Supplementary Table S3**). For ADE specification as shown in **Fig. 1** and **Materials and Methods**, it was necessary to maintain activin A levels, but remove bFGF to reduce active cell-signaling pathways and maintain pluripotency (24). On the other hand, HC requires BMP4 and FGF10 signaling (25). ADE specification and HC require several days to achieve treatment-induced changes in phenotype. Therefore, we treated cells with activin A, and a combination of BMP4 and FGF10 in RPMI medium supplemented with B27 supplement for ADE and HC, respectively, and varied these treatment periods to identify the optimal timing (~1–3 days for ADE and ~1–4 days for HC) for hepatic progenitor cell differentiation by observing the expression levels of genes associated with each differentiation phenotype following treatment by performing quantitative RT-PCR (**Fig. 3A and B**).

Following 1 day of treatment for ADE specification, cells continued to express most of the pluripotency associated genes, including *NANOG*, *SOX2*, and *OCT4* (or *POU5F1*) (**Fig. 3B, "*Pluripotency*"**). When the treatment for ADE specification was extended to 3 days, while the expression levels of pluripotency associated genes was decreased, the genes associated with extraembryonic endoderm (*SOX7*, *LAMB1*, and *HNF1β*), mesoendoderm (*GSC* and *NODAL*), endoderm (*FOXA2*, *SOX17*, *CXCR4*, *HNF1β*, and *HNF4α*), and early hepatic cells (*AFP*, *CYP3A7*,

DLK1, *PROX1*, and *TBX3*) were increased in their expression. Although 1-day treatment for ADE specification did not induce expression of genes associated with hepatic nuclear receptors and/or transporters, expression of these genes was observed on days ~2 and ~3. These results indicated that 3 and 4 days of treatment for ADE and HC, respectively, were optimal to obtain hepatic progenitor cells.

Evaluation of hepatocyte-differentiation status by observing gene-expression patterns

To confirm maturation status, we conducted multiplex quantitative PCR to measure gene expression associated with hepatic differentiation from hPSCs, followed by clustering analysis (**Fig. 4**). Clustering analysis based on gene-expression patterns resulted in six clusters. *Class 1* genes in the undifferentiated cells exhibited the highest expression levels, which decreased after the initiation of differentiation. Most *Class1* genes, including *NANOG*, *SOX2*, and *POU5F1*, were associated with pluripotency. *Class 2* included endoderm genes, such as *CXCR4*, *GATA6*, and *SOX17*, which exhibited peak expression at day 5. *Class 3* included early hepatic genes, such as *DLK1* and *TBX3*, that exhibited peak expression at day 12, as well as some genes associated with the cytochrome P450 (CYP) family (*CYP1A2*, *CYP2D6*, and *CYP2E1*). *Class 4* included many hepatic genes, such as *AHSG*, *APOA4*, and *HNF1A*, as well as hepatic transporter genes and solute-carrier-family genes, such as *SLC10A1*, *SLC22A1*, and *SLC22A2*, and exhibited the highest levels of expression at days 20 or 24. *Class 5* genes, including *AQP1*, *B2M*, *CD9*, *CYP2C8*, *NR3C1*, *SLC22A2*, and *SOX7*, showed the highest expression at day 30, but did not appear to exhibit functional enrichment. *Class 6* showed unique gene-expression patterns, with genes initiating expression on day 20 and peaking at day 35. This includes hepatic genes, such as *ALB*, *SERPINA*, and *TAT*, as well as other early hepatic genes. These gene-expression data suggested that our hepatic differentiation method resulted in a natural developmental process.

Differences in gene expression between hPSC-derived hepatocyte-like cells and liver lysate

To investigate similarities between mature liver and cultured cells, we compared gene-expression patterns between hPSC-derived hepatocyte-like cells and mature liver lysate (**Fig. 5**) using hPSC-derived hepatocyte-like cells at days 0, 24, and 35 of differentiation and liver lysate from a healthy donor. Hepatic marker genes, such as *ALB* and *HNF4A*, exhibited significant increases during the culture process, indicating progression of differentiation and increased similarity between hPSC-derived hepatocyte-like cells and mature liver lysate. Additionally, genes including *AFP*, *APOA4*, *KRT7*, *KRT8*, *KRT18*, *KRT19*, *DLK1*, *GATA6*, and *HNF1B*, exhibited increased expression between days 0 and 24 that were higher than the expression of these genes observed in liver lysate. *AFP* is a marker of hepatoblasts and fetal livers, and *APOA4* exhibits high expression levels in fetal liver. *KRT7*, *KRT8*, *KRT18*, and *KRT19* are expressed in cholangiocytes, *DLK1* is a hepatic progenitor-cell-surface marker, and *GATA6* and *HNF1B* are transcription factors. Specifically, both AFP and DLK1 are strongly expressed in the hPSC-derived cells more than that of liver lysate, resulting these cells did not reach to the level of an matured adult liver. However, genes from the CYP family in hPSC-derived cells exhibited lower expression levels relative to those observed in liver lysate, suggesting that our method requires improvement in terms of CYP expression and activity.

Functions of hPSC-derived hepatocyte-like cells

To confirm the maturity of hPSC-derived hepatocyte-like cells at the protein level, we conducted immunocytochemistry for one of the maturation marker, A1AT (**Fig. 6A and Supplementary Fig. S2**). Hepatocyte-like cells derived from H9 hESCs over 33 days using our method exhibited A1AT expression, as well as the expression of genes associated with the CYP family (e.g., *CYP1A1*, *CYP2A9*, and *CYP2C19*), transporters (*MRP2* and *MDR/TAP*), hepatic enzymes (*UGT1A1*, *A1AT*, and *TDO1*), and a transcription factor (*HNF1α*) (**Fig. 6B**). Controls for these experiments included HepG2 hepatocellular carcinoma cells and liver extracts from a healthy donor. Undifferentiated H9 hESCs did not express hepatic markers; however, hepatocyte-like cells

derived from H9 hESCs expressed all marker genes tested. By contrast, HepG2 cells did not express *CYP2A9*, *CYP2C19*, *MDR/TAP*, *UGT1A1*, or *TDO1*. As expected, the liver extract from the healthy donor strongly expressed all tested genes at levels exceeding those of hepatocyte-like cells derived from H9 hESCs. These results indicated that hepatocyte-like cells derived from H9 hESCs exhibited improved gene-expression relative to a HepG2 cell line, but were unable to match levels observed in liver extracts from a healthy donor.

To evaluate drug uptake and excretion, we used ICG as a non-invasive marker of drug uptake and excretion in the liver (26, 27) (**Fig. 6C and Supplementary Fig. S3**). After 24 days following hPSC hepatic differentiation, ICG was incubated with hPSC-derived hepatocytes for 1 h to visualize ICG uptake. After 24 h, cells were also evaluated to determine ICG excretion. Cells (10%) showed effective ICG uptake and excretion; thereby confirming the functional viability of the hPSC-derived hepatocyte-like cells.

Maturation of hPSC-derived hepatocyte-like cells using a microfluidic 3D-culture device

To facilitate maturation levels, we developed a simple 3D-culture method using a microfluidic device. We hypothesized that 3D-culture conditions would provide a more suitable environment for hepatocytes as compared with conventional two-dimensional (2D)-culture methods (6) towards mimicking 3D micro liver tissues (**Fig. 7A**). Previously, we reported the microfluidic device enabling 3D culture of hPSCs (9, 10) (**Fig. 7B**), and utilized to perform 3D culturing of hepatocyte-like cells from day 12 to enhance the maturation process, in this study. The microfluidic device was made of PDMS, which exhibits good biocompatibility and gas permeability (28), and contained two microfluidic 3D cell-culture chambers [10 mm (L) × 1.5 mm (W) × 150 μm (H)] with a cell inlet (0.75-mm diameter) and medium reservoir (3-mm diameter). Our results indicated that the A1AT hepatocyte-maturation marker was more strongly expressed in 3D-cultured hepatocyte-like cells derived from H9 hESCs as compared with levels observed in 2D-cultured cells (**Fig. 7C**). In terms of gene expression, we also confirmed increased expression of other

hepatocyte-marker genes, such as *UGT1A1*, *CYP3A4*, *CYP2A9*, *CYC2C19*, and *CYP2D6*, in the 3D-cultured H9 hESC-derived hepatocyte-like cells relative to levels observed in 2D-cultured cells (**Fig. 7D**). To investigate differences in functionality, an ICG uptake/excretion assay was performed on cells from both 3D- and 2D cultures (**Fig. 7E**). Interestingly, >90% of 3D-cultured cells showed ICG uptake within 1 h, with most cells also effectively excreting the ICG after 24 h.

Conclusion

In this study, we developed an efficient and robust method to induce hPSC differentiation into functional hepatocyte-like cells. By optimizing the basal medium, a combination of chemicals, and initial cell-seeding density for endoderm differentiation, we obtained endoderm-differentiated cells with a homogeneous population highly expressing CXCR4 from dissociated hPSCs. Additionally, we optimized the periods required for ADE specification and HC according to quantitative PCR analysis. This is the first demonstration of application of a microfluidic 3D cell-culture platform for the maturation of hepatocyte-like cells.

Hepatocytes are important cells for drug screening and chemical-safety testing in a variety of industries, including cosmetics and agriculture. However, there are limited numbers of primary hepatocytes available, with these numbers varying by donor. Even after the acquisition of primary hepatocytes, current 2D-culture conditions do not allow for their continued differentiation into functional cells. Although current hepatocyte cell lines, such as HepG2, have been used as alternatives, they often show different characteristics from primary hepatocytes. Here, we developed a method using hPSCs and microfluidic 3D culture to obtain sufficient amounts of functional hepatocyte-like cells. We envision that our method will fulfill current requirements from the fields of regenerative medicine and drug discovery.

Acknowledgments

Funding was generously provided by the Japan Society for the Promotion of Science (JSPS; 24656502, 26560209, and 16K14660). Funding was also provided by the Terumo Life Science Foundation. The WPI-iCeMS is supported by the World Premier International Research Centre Initiative (WPI), MEXT, Japan.

Conflict of interests

Kyoto University (K.K. and M.Y.) filed a provisional Japanese patent application based on the research presented herein.

References

1. Thomson, J.A., Itskovitz-Eldor, J., Shapiro, S.S., Waknitz, M.A., Swiergiel, J.J., Marshall, V.S., andJones, J.M. Embryonic stem cell lines derived from human blastocysts. Science **282**, 1145, 1998.

2. Yu, J., Vodyanik, M.A., Smuga-Otto, K., Antosiewicz-Bourget, J., Frane, J.L., Tian, S., Nie, J., Jonsdottir, G.A., Ruotti, V., Stewart, R., Slukvin, II, andThomson, J.A. Induced pluripotent stem cell lines derived from human somatic cells. Science **318**, 1917, 2007.

3. Greenhough, S., Bradburn, H., Gardner, J., andHay, D.C. Development of an embryoid body-based screening strategy for assessing the hepatocyte differentiation potential of human embryonic stem cells following single-cell dissociation. Cellular reprogramming **15**, 9, 2013.

4. Inamura, M., Kawabata, K., Takayama, K., Tashiro, K., Sakurai, F., Katayama, K., Toyoda, M., Akutsu, H., Miyagawa, Y., Okita, H., Kiyokawa, N., Umezawa, A., Hayakawa, T., Furue, M.K., andMizuguchi, H. Efficient generation of hepatoblasts from human ES cells and iPS cells by transient overexpression of homeobox gene HEX. Molecular therapy : the journal of the American Society of Gene Therapy **19**, 400, 2011.

5. Takayama, K., Inamura, M., Kawabata, K., Tashiro, K., Katayama, K., Sakurai, F., Hayakawa, T., Furue, M.K., andMizuguchi, H. Efficient and directive generation of two distinct endoderm lineages from human ESCs and iPSCs by differentiation stage-specific SOX17 transduction. PloS one **6**, e21780, 2011.

6. Schepers, A., Li, C., Chhabra, A., Seney, B.T., andBhatia, S. Engineering a perfusable 3D human liver platform from iPS cells. Lab Chip **16**, 2644, 2016.

7. Kruitwagen, H.S., Oosterhoff, L.A., Vernooij, I., Schrall, I.M., van Wolferen, M.E., Bannink, F., Roesch, C., van Uden, L., Molenaar, M.R., Helms, J.B., Grinwis, G.C.M., Verstegen, M.M.A., van der Laan, L.J.W., Huch, M., Geijsen, N., Vries, R.G., Clevers, H., Rothuizen, J., Schotanus, B.A., Penning, L.C., andSpee, B. Long-Term Adult Feline Liver Organoid Cultures for Disease Modeling of Hepatic Steatosis. Stem cell reports **8**, 822, 2017.

8. Asai, A., Aihara, E., Watson, C., Mourya, R., Mizuochi, T., Shivakumar, P., Phelan, K., Mayhew, C., Helmrath, M., Takebe, T., Wells, J., andBezerra, J.A. Paracrine signals regulate human liver organoid maturation from induced pluripotent stem cells. Development **144**, 1056, 2017.

9. Kamei, K.I., Koyama, Y., Tokunaga, Y., Mashimo, Y., Yoshioka, M., Fockenberg, C., Mosbergen, R., Korn, O., Wells, C., andChen, Y. Characterization of Phenotypic and Transcriptional Differences in Human Pluripotent Stem Cells under 2D and 3D Culture Conditions. Advanced healthcare materials **5**, 2951, 2016.

10. Kamei, K., Mashimo, Y., Koyama, Y., Fockenberg, C., Nakashima, M., Nakajima, M., Li, J.J., andChen, Y. 3D printing of soft lithography mold for rapid production of polydimethylsiloxane-based microfluidic devices for cell stimulation with concentration gradients. . Biomed Microdevices **17**2015.

11. Wilkerson, M.D., andHayes, D.N. ConsensusClusterPlus: a class discovery tool with confidence assessments and item tracking. Bioinformatics **26**, 1572, 2010.

12. Hay, D.C., Fletcher, J., Payne, C., Terrace, J.D., Gallagher, R.C., Snoeys, J., Black, J.R., Wojtacha, D., Samuel, K., Hannoun, Z., Pryde, A., Filippi, C., Currie, I.S., Forbes, S.J., Ross, J.A., Newsome, P.N., andIredale, J.P. Highly efficient differentiation of hESCs to functional hepatic endoderm requires ActivinA and Wnt3a signaling. Proceedings of the National Academy of Sciences of the United States of America **105**, 12301, 2008.

13. Basma, H., Soto-Gutierrez, A., Yannam, G.R., Liu, L., Ito, R., Yamamoto, T., Ellis, E., Carson, S.D., Sato, S., Chen, Y., Muirhead, D., Navarro-Alvarez, N., Wong, R.J., Roy-Chowdhury, J., Platt, J.L., Mercer, D.F., Miller, J.D., Strom, S.C., Kobayashi, N., andFox, I.J. Differentiation and transplantation of human embryonic stem cell-derived hepatocytes. Gastroenterology **136**, 990, 2009.

14. Rossi, J.M., Dunn, N.R., Hogan, B.L., andZaret, K.S. Distinct mesodermal signals, including BMPs from the septum transversum mesenchyme, are required in combination for hepatogenesis from the endoderm. Genes & development **15**, 1998, 2001.

15. Bone, H.K., Nelson, A.S., Goldring, C.E., Tosh, D., andWelham, M.J. A novel chemically directed route for the generation of definitive endoderm from human embryonic stem cells based on inhibition of GSK-3. Journal of cell science **124**, 1992, 2011.

16. Si-Tayeb, K., Noto, F.K., Nagaoka, M., Li, J., Battle, M.A., Duris, C., North, P.E., Dalton, S., andDuncan, S.A. Highly efficient generation of human hepatocyte-like cells from induced pluripotent stem cells. Hepatology **51**, 297, 2010.

17. Jung, J., Zheng, M., Goldfarb, M., andZaret, K.S. Initiation of mammalian liver development from endoderm by fibroblast growth factors. Science **284**, 1998, 1999.

18. Huang, T.S., Li, L., Moalim-Nour, L., Jia, D., Bai, J., Yao, Z., Bennett, S.A., Figeys, D., andWang, L. A Regulatory Network Involving beta-Catenin, E-Cadherin, PI3K/Akt, and Slug Balances Self-Renewal and Differentiation of Human Pluripotent Stem Cells in Response to Wnt Signaling. Stem cells 2014.

19. Mathew, S., Sundararaj, S., Mamiya, H., andBanerjee, I. Regulatory interactions maintaining self-renewal of human embryonic stem cells as revealed through a systems analysis of PI3K/AKT pathway. Bioinformatics **30**, 2334, 2014.

20. Watanabe, K., Ueno, M., Kamiya, D., Nishiyama, A., Matsumura, M., Wataya, T., Takahashi, J.B., Nishikawa, S., Nishikawa, S., Muguruma, K., andSasai, Y. A ROCK inhibitor permits survival of dissociated human embryonic stem cells. Nature biotechnology **25**, 681, 2007.

21. Ludwig, T.E., Bergendahl, V., Levenstein, M.E., Yu, J., Probasco, M.D., andThomson, J.A. Feeder-independent culture of human embryonic stem cells. Nat Methods **3**, 637, 2006.

22. Hannan, N.R., Segeritz, C.P., Touboul, T., andVallier, L. Production of hepatocyte-like cells from human pluripotent stem cells. Nature protocols **8**, 430, 2013.

23. Nakagawa, M., Koyanagi, M., Tanabe, K., Takahashi, K., Ichisaka, T., Aoi, T., Okita, K., Mochiduki, Y., Takizawa, N., andYamanaka, S. Generation of induced pluripotent stem cells without Myc from mouse and human fibroblasts. Nature biotechnology **26**, 101, 2008.

24. Festuccia, N., Osorno, R., Wilson, V., andChambers, I. The role of pluripotency gene regulatory network components in mediating transitions between pluripotent cell states. Curr Opin Genet Dev **23**, 504, 2013.

25. Shin, D., andMonga, S.P. Cellular and molecular basis of liver development. Compr Physiol **3**, 799, 2013.

26. Ishikawa, T., Kobayashi, M., Yanagi, S., Kato, C., Takashima, R., Kobayashi, E., Hagiwara, K., andOchiya, T. Human induced hepatic lineage-oriented stem cells: autonomous specification of human iPS cells toward hepatocyte-like cells without any exogenous differentiation factors. PloS one **10**, e0123193, 2015.

27. Takayama, K., Inamura, M., Kawabata, K., Sugawara, M., Kikuchi, K., Higuchi, M., Nagamoto, Y., Watanabe, H., Tashiro, K., Sakurai, F., Hayakawa, T., Furue, M.K., andMizuguchi, H. Generation of metabolically functioning hepatocytes from human pluripotent stem cells by FOXA2 and HNF1alpha transduction. Journal of hepatology **57**, 628, 2012.

28. Kamei, K., Hirai, Y., Yoshioka, M., Makino, Y., Yuan, Q., Nakajima, M., Chen, Y., andTabata, O. Phenotypic and transcriptional modulation of human pluripotent stem cells induced by nano/microfabrication materials. Advanced healthcare materials **2**, 287, 2013.

Figure Legends

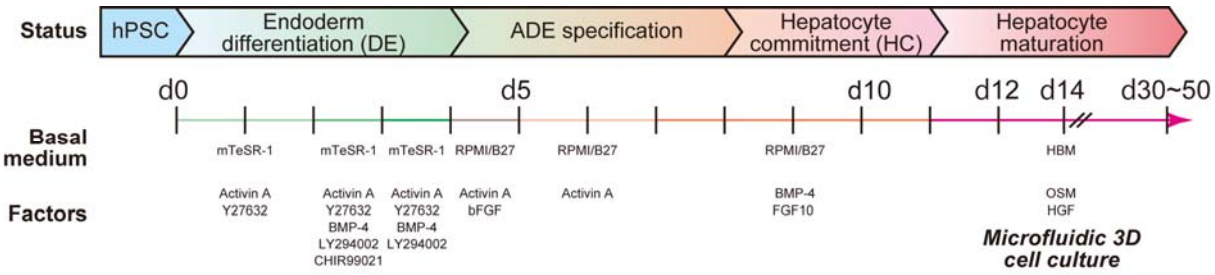

FIG. 1. The hepatic differentiation process from human pluripotent stem cells. A variety of solutions containing basal media, growth factors, and chemicals were administered to hPSCs to efficiently induce differentiation to hepatocyte-like cells.

ADE, anterior definitive endoderm; DE, definitive endoderm; hPSC, human pluripotent stem cell; HC, hepatocyte commitment.

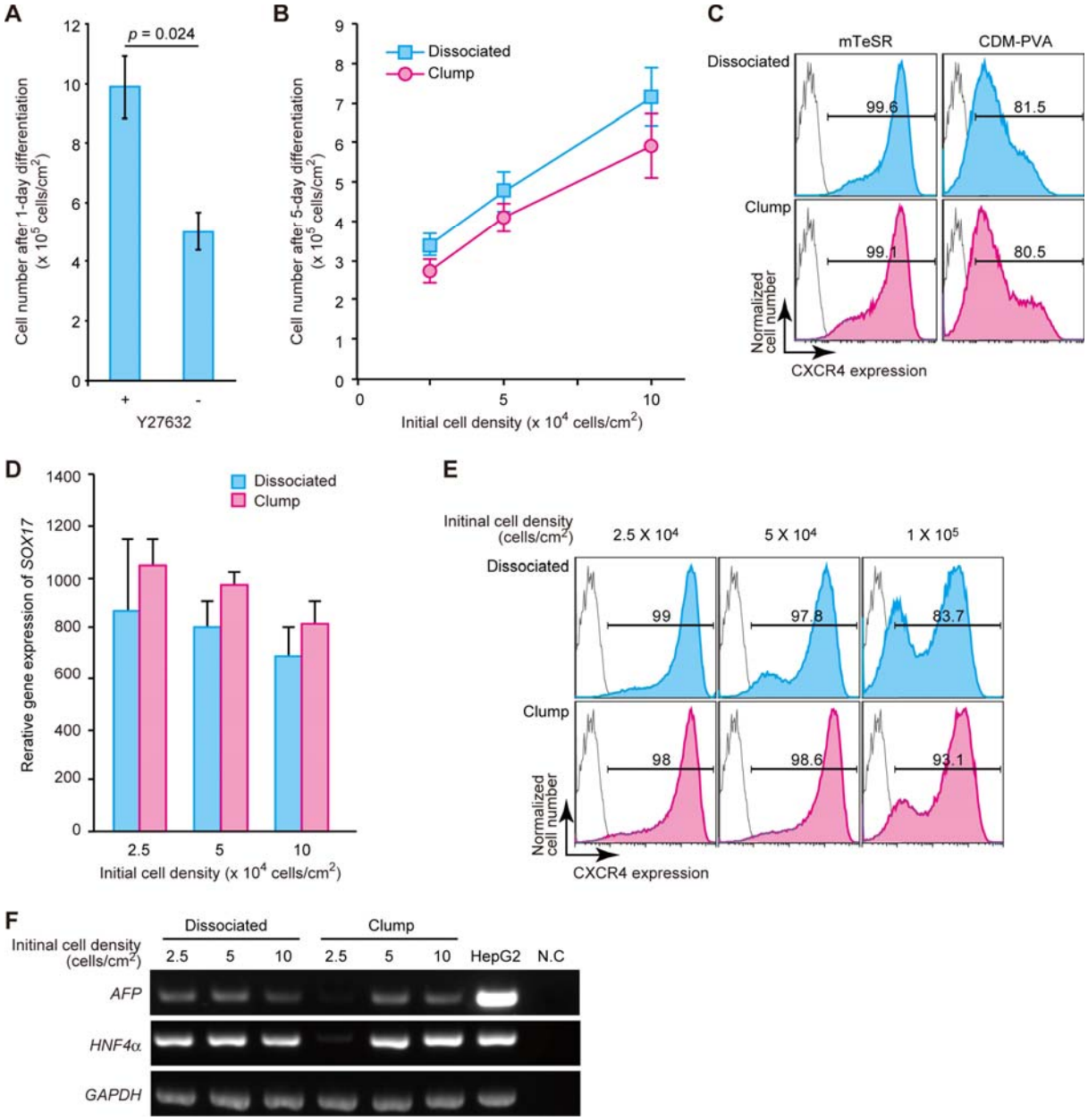

FIG. 2. A combination of ROCK (10 μM Y27632) and PI3K (10 μM LY294002) inhibitors facilitate survival and inhibit self-renewal of hPSCs. (**A**) 1-day treatment with mTeSR-1 basal medium in combination with a ROCK inhibitor increases cell survival of H9 human embryonic stem cells (hESCs). Each bar and error bar represents the mean ± standard deviation (n = 3). (**B, C**) Both dissociated and clumped H9 hESCs treated with mTeSR-1/Y27632 were able to proliferate during definitive-endoderm (DE) differentiation (**B**) with similar doubling times (**C**). Each bar and error bar represents the mean ± standard deviation (n = 3). "n.s." represents "not significant". (**D**) Selection of basal medium to induce differentiation of dissociated or clumped hESCs into DE by

monitoring the expression levels of the CXCR4 DE marker. Cells treated with mTeSR-1 medium supplemented with activin A, BMP-4, LY294002, and CHIR99021, and Y27632 showed a more homogeneous cell population with higher CXCR4 expression. (**E**) Initial cell density is inversely correlated with the expression levels of the *SOX17* DE marker. At low initial cell density, *SOX17* expression levels varied among experiments. Each bar represents the mean ± standard deviation (*n* = 3). (**F**) Representative gel electrophoresis of RT-PCR samples to derive mRNA expression of differentiation markers of α-fetoprotein (*AFP*) and hepatocyte nuclear factor 4α (*HNF4α*) on day 12. *GAPDH,* a housekeeping gene, was used as an internal control, obtained from three independent experiments.

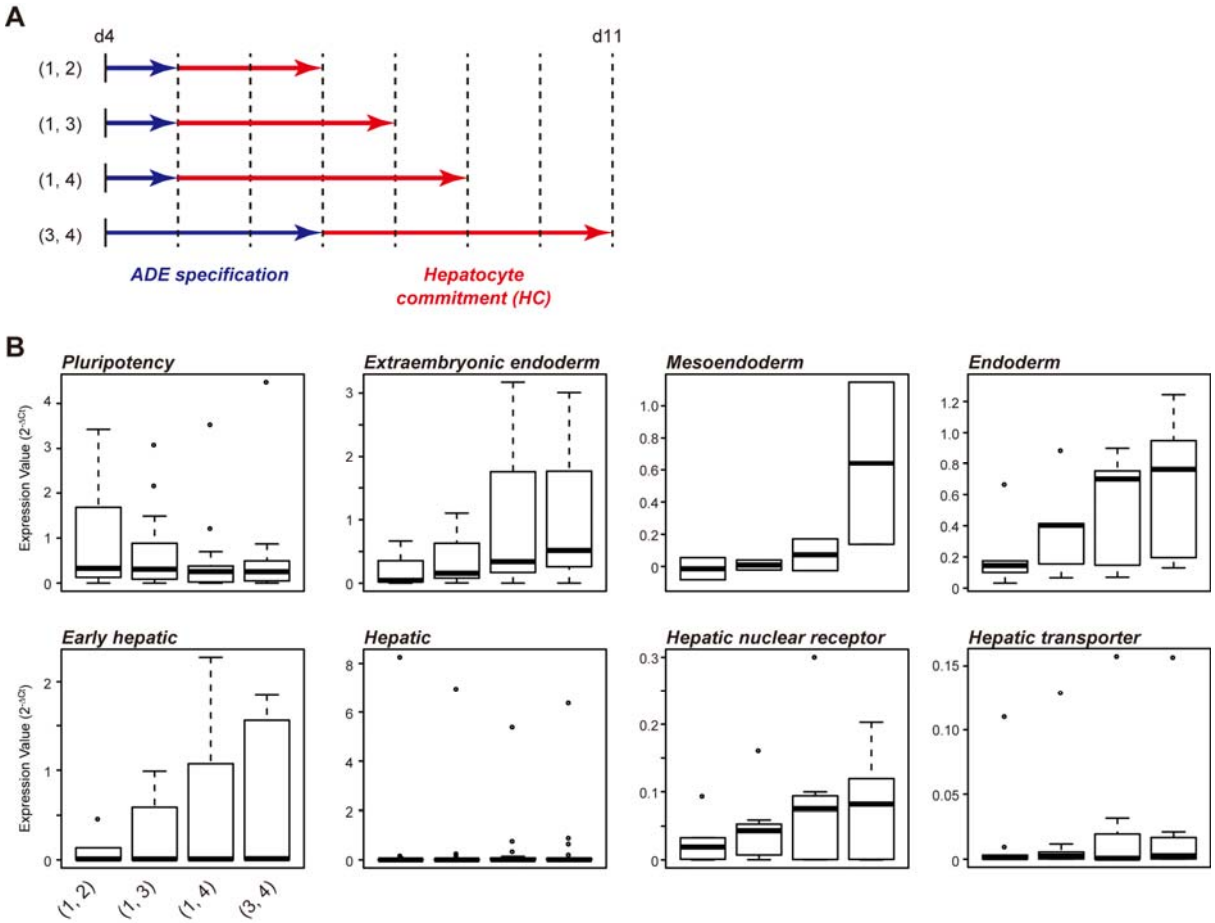

FIG. 3. Quantitative RT-PCR analysis revealed optimal periods for anterior definitive endoderm (ADE) specification and hepatocyte commitments. (**A**) Tested periods for ADE specification and hepatocyte commitments. (**B**) Gene-expression patterns of 253G1 hiPSCs treated for ADE specification and hepatocyte commitments. (1, 2) represents 1-day treatment of ADE specification and 2-day treatment for hepatocyte commitments. Center lines show the medians; box limits indicate 25% and 75%; whiskers extend 1.5 times the interquartile range from 25% and 75%. These experiments were carried out at least three times independently.

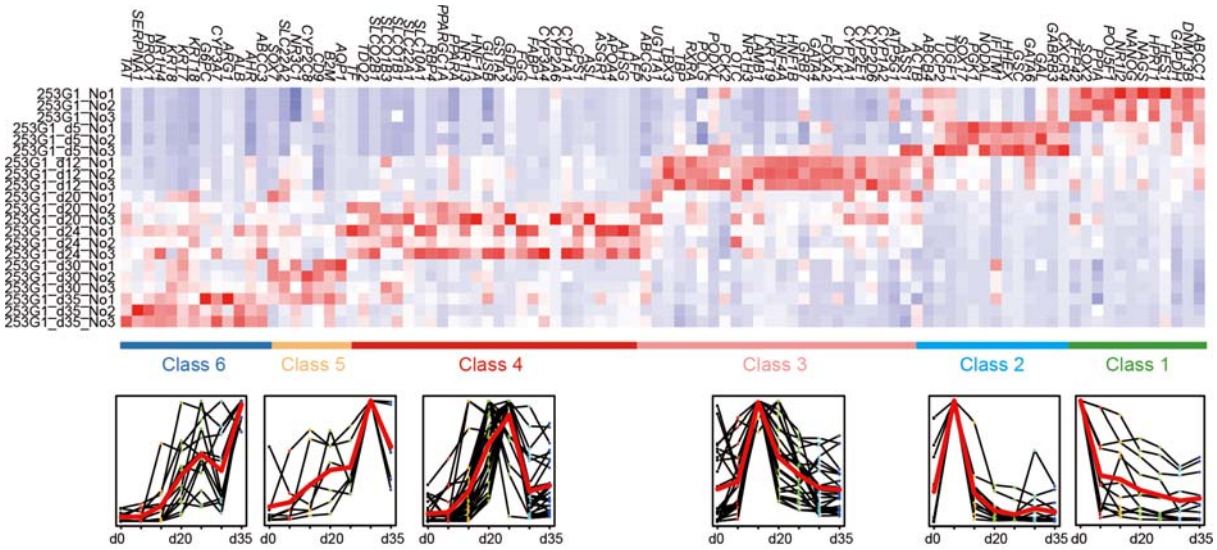

FIG. 4. Gene-expression analysis investigating the overall gene-expression signatures from pluripotent status to hepatocyte differentiation. Clustering analysis based on 96 gene expression patterns divided the tested genes into six clusters. An expression trend for each group during the hepatocyte-differentiation process was also plotted.

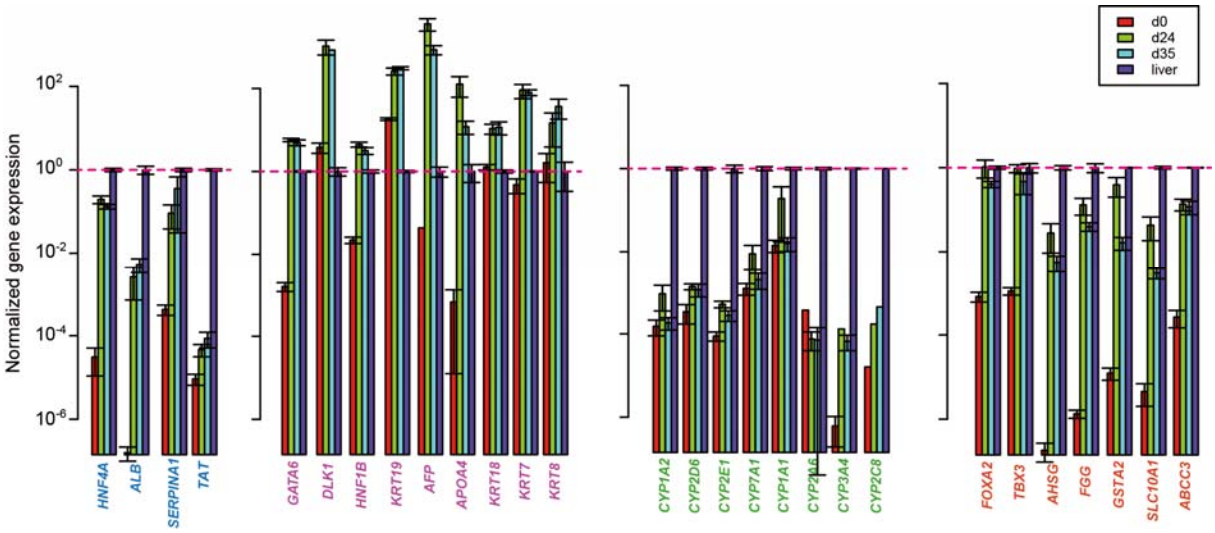

FIG. 5. Comparison of gene-expression patterns between hepatocyte-like cells derived from 253G1 hiPSCs and liver lysate. Genes associated with hepatic, hepatoblast, and cytochrome P450 (CYP) family genes were measured by quantitative RT-PCR. Gene-expression values were normalized using the values from liver lysate genes as standards. These experiments were carried out at least three times independently.

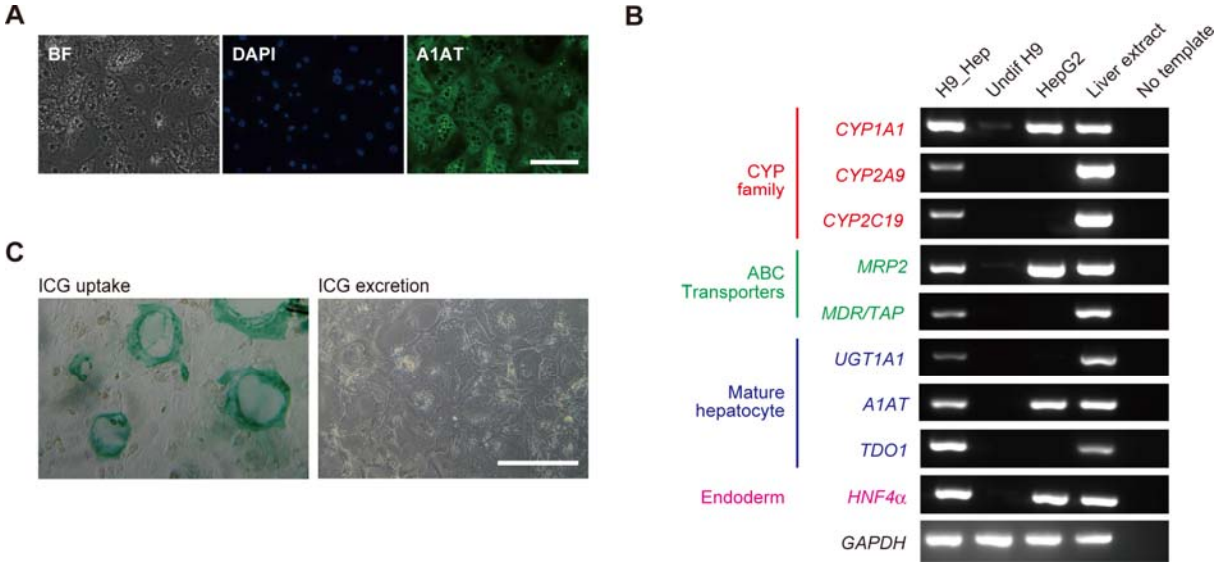

FIG. 6. Functional assays for hepatocyte-like cells derived from hPSCs. (**A**) Immunocytochemistry to visualize hepatocyte-maturation marker α1 anti-trypsin (A1AT) in hepatocyte-like cells derived from H9 hESCs following a 33-day treatment. Scale bar represents 20 µm. (**B**) Representative gel electrophoresis of RT-PCR products from mRNAs associated with the cytochrome P450 (CYP) family (e.g., *CYP1A1*, *CYP2A9*, and *CYP2C19*), ATP-binding cassette (ABC) transporters (*MRP2* and *MDR/TAP*), hepatocyte-maturation markers (*UGT1A1*, *A1AT*, and *TDO1*), and endoderm markers (*HNF1α*), obtained from independently triplicated experiments. HepG2 hepatocellular carcinoma cells were used as a control, and a liver extract from a healthy donor was used as a positive control. H9_Hep and Undif_H9 represent hepatocyte-like cells derived from H9 hESCs and undifferentiated H9 hESCs, respectively. (**C**) Microphotographs of hepatocyte-like cells treated with indocyanine green (ICG) for 1 h to visualize ICG uptake and then excretion after 24 h. Scale bar represents 100 µm.

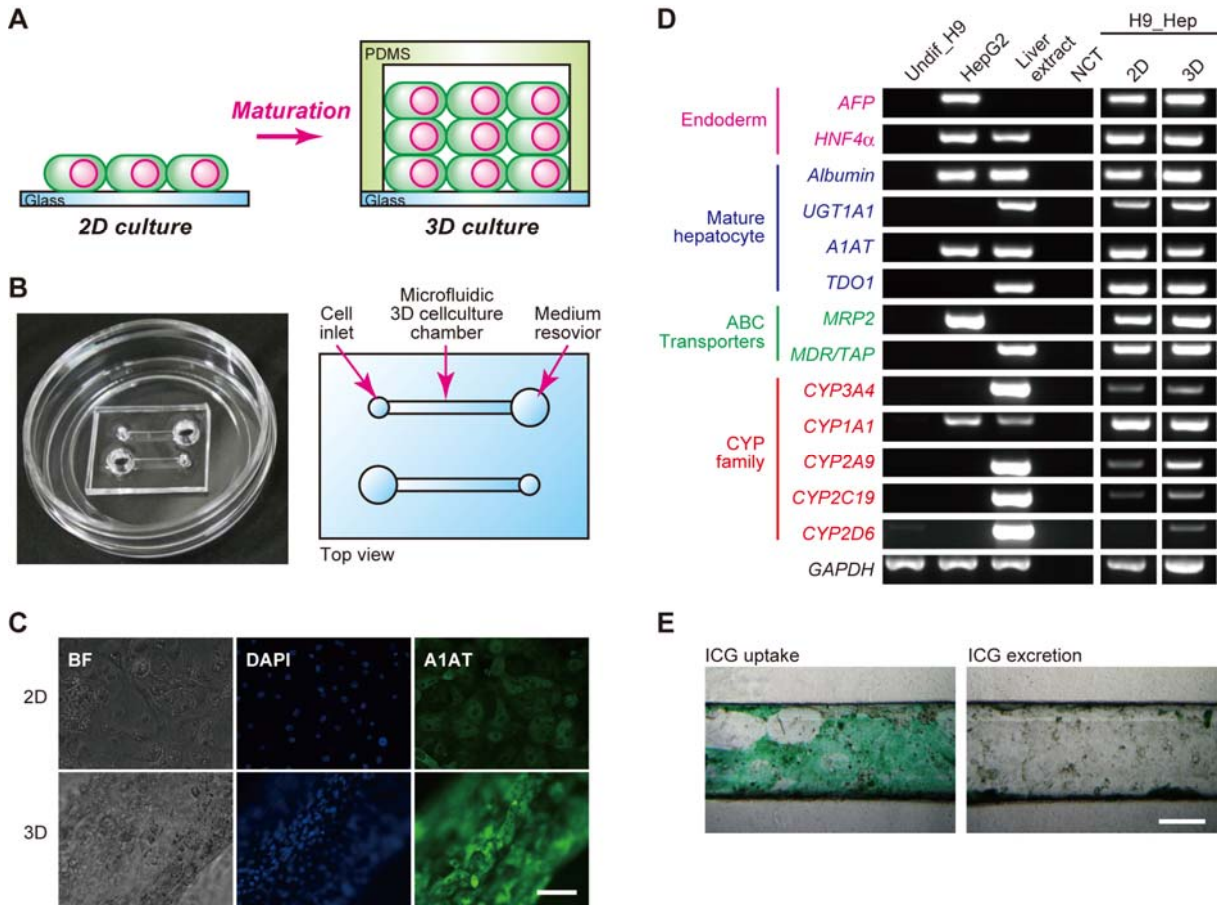

FIG. 7. A microfluidic 3D-culture device facilitates maturation of hPSC-derived hepatocyte-like cells. (**A**) Illustration of 2D and microfluidic 3D cultures for hepatocyte maturation. (**B**) Photograph of a microfluidic 3D-culture device (10) and the structure of a microfluidic cell-culture chamber [10 mm (L) × 1.5 mm (W) × 150 µm (H)] with a cell inlet (0.75-mm diameter) and medium reservoir (3-mm diameter). (**C**) Immunocytochemistry to visualize the hepatocyte-maturation marker α1 anti-trypsin (A1AT) in H9 hESC-derived hepatocyte-like cells. "2D" and "3D" represent hepatocyte-like cells derived from H9 hESCs cultured in a conventional 35-mm culture dish and a microfluidic 3D cell-culture device, respectively. Scale bar represents 20 µm. (**D**) Representative gel electrophoresis of RT-PCR products for mRNAs associated with the cytochrome P450 family (e.g., *CYP3A4*, *CYP1A1*, *CYP2A9*, *CYP2C19*, and *CYP2D6*), ATP-binding cassette (ABC) transporters (*MRP2* and *MDR/TAP*), hepatocyte-maturation markers (*Albumin*, *UGT1A1*, *A1AT*, and *TDO1*), and endoderm markers (*AFP* and *HNF1α*), obtained from independently triplicated

experiment. HepG2 hepatocellular carcinoma cells were used as a control, and a liver extract from a healthy donor was used as a positive control. H9_Hep and Undif_H9 represent hepatocyte-like cells derived from H9 hESCs and undifferentiated H9 hESCs, respectively. (**E**) Microphotographs of hepatocyte-like cells treated with indocyanine green (ICG) for 1 h to visualize ICG uptake and then excretion after 24 h. Scale bar represents 500 µm.